

Magnetic transitions in dysprosium: A specific-heat study

K. D. Jayasuriya, S. J. Campbell,* and A. M. Stewart

Department of Solid State Physics, Research School of Physical Sciences, Australian National University, Canberra, ACT 2601, Australia

(Received 11 May 1984)

The magnetic transitions of the heavy rare-earth metal dysprosium have been examined by specific-heat measurements using a small single crystal (0.6782 g) and a large polycrystalline sample (43.25 g). A value for the latent heat of $39.1 \pm 1.5 \text{ J mol}^{-1}$ is obtained at the discontinuous transition from ferromagnetism to helical antiferromagnetism, and a temperature hysteresis of $1.2 \pm 0.4 \text{ K}$ is observed at this transition. The data around the continuous transition from helical antiferromagnetism to paramagnetism at the Néel temperature $T_N = 179.90 \pm 0.18 \text{ K}$ have been analyzed in terms of the equation $C^\pm = (A^\pm/\alpha^\pm)|t|^{-\alpha^\pm} (1 + E^\pm|t|^{x^\pm}) + B^\pm + D^\pm t$, where $t = (T - T_N)/T_N$. Agreement to within two standard errors was obtained for the critical parameters of the single-crystal and polycrystalline data. The value of the critical exponent α obtained from the data of the single crystal is 0.24 ± 0.02 , whereas that obtained from the data of the polycrystalline sample is 0.14 ± 0.05 . We find that the scaling law $\alpha^+ = \alpha^-$ is valid for the dysprosium critical data. In order for the condition $B^+ = B^-$, predicted by theory, to be satisfied we found it necessary to include the confluent singular term in E in our fit. The values of α that we obtain are not close to the predictions of renormalization-group theory for magnetic systems with short-range exchange interactions.

I. INTRODUCTION

We have recently reported detailed studies of the dc specific heat of the rare-earth metals terbium¹ and holmium² in the regions of their magnetic transitions at the Néel temperatures. Here we report a specific-heat study of the magnetic transitions in the rare-earth metal dysprosium. Dysprosium, which has magnetic properties very similar to terbium, exhibits two magnetic transitions: a transition from paramagnetism to an incommensurate helical antiferromagnetic state at the Néel temperature $T_N \sim 178.5 \text{ K}$, and a transition from this incommensurate state to ferromagnetism at the Curie temperature $T_C \sim 85 \text{ K}$ (Ref. 3).

Although there are several reports of the low-temperature specific heat of dysprosium in the literature (e.g., 0.25–2 K, Dash *et al.*;⁴ 0.4–4 K, Lounasmaa and Guenther;⁵ 3–25 K, Lounasmaa and Sundstrom⁶), there is no clear agreement between the results, and the behavior of the specific heat of dysprosium at low temperatures is not yet clearly understood.⁷ This is attributed to the unavailability of accurate low-temperature specific-heat measurements on high-purity specimens.

Specific-heat measurements of dysprosium around the Néel temperature T_N have been carried out by five investigators,^{8–12} and critical parameters for a small (mass not stated) single crystal of dysprosium¹⁰ and for small ($m = 0.140$ and 0.675 g) dysprosium specimens¹² (not stated whether single crystals or polycrystalline specimens) have been reported in the literature. The only dc specific-heat measurement of dysprosium around the Curie temperature T_C has been carried out on a polycrystalline sample.⁸ No value for the latent heat associated with the discontinuous transition at T_C of dysprosium has been

obtained from a direct calorimetric measurement by any of the above workers.

In the present paper we report measurements of the specific heat of dysprosium around the regions of the magnetic transitions including an analysis of the critical parameters at the Néel point. These measurements were carried out on a small single crystal (0.6782 g) and a large polycrystalline sample (43.25 g) of dysprosium.

II. EXPERIMENT

The measurements were made with the adiabatic calorimeter described previously.² The absolute accuracy of the measurements of specific heat is estimated to be better than $\pm 0.3\%$ for samples of large heat capacity (e.g., a copper sample of 50 g, 19 J K^{-1}) reducing to $\pm 3\%$ for samples of small heat capacity (e.g., a copper sample of 1.8 g, 0.7 J K^{-1}). The heat capacity of the dysprosium single crystal used in this study is $\sim 0.18 \text{ J K}^{-1}$ (at 150 K). As the single crystal has a heat capacity much smaller than that which the calorimeter was designed to measure ($\sim 2 \text{ J K}^{-1}$) the absolute accuracy of the results for the single crystal are not expected to be better than $\pm 10\%$. In practice, as described below, we observe deviations of $< 6\%$ from the absolute values of earlier workers with a scatter in the present data of $< 0.5\%$. We might also expect effects to be present that are associated with thermal time constants of the relatively large addenda. These might be expected to be largest when the specific heat is changing most rapidly, i.e., at the transition. The heat capacity of the polycrystalline dysprosium sample used in this study is $\sim 12 \text{ J K}^{-1}$ (at 150 K), and so the absolute accuracy of the specific-heat measurements on the

polycrystalline dysprosium sample was expected to be around $\pm 0.3\%$.

The dysprosium single crystal was prepared at the Ames Laboratory, Iowa by the metallothermic method.¹³ The purity of the crystal is 99.63 at. % (99.98 wt. %), the principal impurities being hydrogen, oxygen, carbon, tantalum, iron, lead, nitrogen, and bromine. A value for the resistivity ratio of this single crystal is not available. The single-crystal sample has a cylindrical shape of length 12.0 mm, and diameter 3.1 mm, with the magnetically easy hexagonal a axis parallel to the axis of the cylinder. The polycrystalline dysprosium sample was taken from the source of the dysprosium sample used by McKenna *et al.*,¹⁴ which was supplied by CERAC Inc. The purity of this polycrystalline sample is 92 at. % (99.3 wt. %), the principal impurities being oxygen, nitrogen, hydrogen, and yttrium. The resistivity ratio $\rho(300\text{ K})/\rho(4.2\text{ K})$ of this polycrystalline sample is about 10. The polycrystalline dysprosium sample has an approximately cylindrical shape of length 27.3 mm and diameter 15.4 mm.

III. SPECIFIC HEAT

A. Results for the single crystal

Several experiments were performed on the single crystal of dysprosium; different warming rates in the range $1.8\text{--}4.3\text{ K h}^{-1}$ (as measured at 150 K) were used. Figure 1 shows typical results for the specific heat of the dysprosium single crystal over the temperature range 75–225 K. The earlier results of Griffel *et al.*⁸ on a polycrystalline dysprosium sample of mass 256.7 g and the results of Amitin *et al.*⁹ are also shown in Fig. 1. No details of the specimen used by Amitin *et al.*⁹ are given in their paper.

The scatter of the data of the present results is better than $\pm 0.5\%$ (Fig. 1). The reproducibility of the results was better than about 1% and no significant dependence

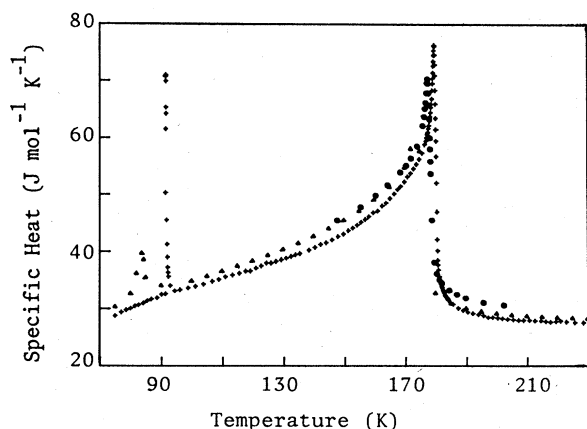


FIG. 1. Results of a typical warming experiment, in this case at a warming rate of 1.8 K h^{-1} as measured at 150 K, showing specific-heat measurements (+) for the dysprosium single crystal. For clarity only one in twelve of the data points is plotted in the regions away from the transitions. Closed triangles (\blacktriangle) and closed circles (\bullet) denote the results of Griffel *et al.* (Ref. 8) and Amitin *et al.* (Ref. 9), respectively.

of the results on the warming rate was observed. As can be seen in Fig. 1, the present results are lower by about 5.5% in the range 100–170 K and by about 2% in the range 190–230 K than the earlier results.

B. Results for the polycrystalline sample

Three experiments were carried out on the polycrystalline dysprosium sample with warming rates in the range $1.7\text{--}3.2\text{ K h}^{-1}$ (as measured at 150 K). Typical results obtained for the specific heat of the polycrystalline dysprosium sample over the temperature 75 to 400 K are shown in Fig. 2. Again for comparison the earlier results of Griffel *et al.*⁸ and Amitin *et al.*⁹ are also shown in Fig. 2. The scatter of the data of the present results is better than $\pm 0.2\%$ and the reproducibility of the results was better than $\pm 0.2\%$. As can be seen in Fig. 2, the earlier results of Griffel *et al.*⁸ and Amitin *et al.*⁹ differ from the present results showing deviations of about +3.5% in the range 100–180 K and about -1% in the range 190–300 K.

C. Nature of the transitions in dysprosium

As for terbium,¹ the essential difference in the nature of the transitions is demonstrated by the graphs of sample temperature against time in Fig. 3, which shows the results obtained for the single-crystal sample around T_C and T_N during a warming run at constant power input. The plateaulike behavior around T_C enables the latent heat at this discontinuous transition to be determined (see below). In contrast only a weak inflection is observed in the graph of temperature against time for the continuous transition around T_N . As for terbium¹ and holmium² we consider that these data distinguish clearly between the nature of the transitions, and that the transition at T_N is not discontinuous as proposed recently by Barak and Walker¹⁵ on the basis of an analysis of the symmetry of the ordered phase. Measurements of Tindall and Stein-

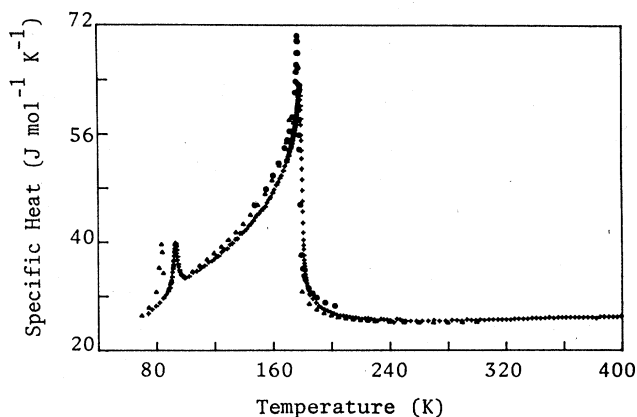


FIG. 2. Specific heat (+) of the dysprosium polycrystalline sample obtained with a warming rate of 2.1 K h^{-1} (as measured at 150 K). For clarity only one in fifteen of the data points is plotted in the regions away from the transitions. Closed triangles (\blacktriangle) and closed circles (\bullet) denote the results of Griffel *et al.* (Ref. 8) and Amitin *et al.* (Ref. 9), respectively.

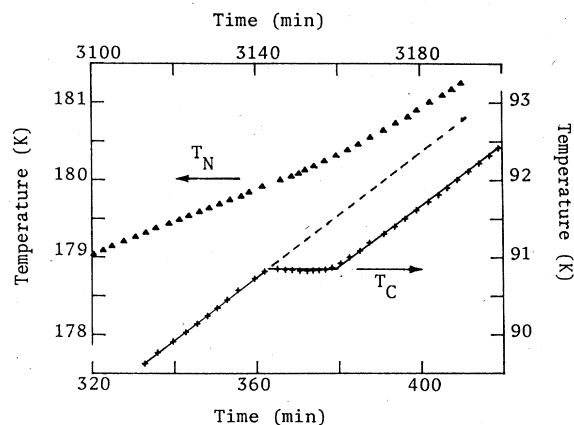


FIG. 3. Temperature of the dysprosium single crystal as a function of time in the regions of the transitions during a warming experiment (rate 1.8 K h^{-1} at 150 K) at constant power input. The apparent transition temperatures T_C and T_N are indicated.

itz¹⁶ did not show a discontinuity in the thermal-expansion coefficient of dysprosium at T_N indicating that the transition at T_N is continuous, in agreement with the present results.

IV. DISCONTINUOUS TRANSITION AT THE CURIE POINT

A. Hysteresis

In order to test for the existence of a thermal hysteresis at T_C in dysprosium, cooling experiments were carried out on the dysprosium single crystal. The same method used for the cooling experiments on the terbium single crystal¹⁷ was employed for the dysprosium single crystal. The present measurements proved more difficult than those on the terbium crystal for two reasons: (i) the transition temperatures T_C and T_N are spaced very widely in dysprosium ($T_N - T_C = \sim 89 \text{ K}$) compared with terbium ($T_N - T_C = \sim 8 \text{ K}$) and it was not possible to maintain an approximately constant heat leak from the dysprosium single crystal during a cooling run; (ii) since the base temperature of the calorimeter is 77 K and the Curie temperature of dysprosium is 91 K , it was not possible to cool the specimen below T_C by maintaining a rotary pump vacuum in the calorimeter while it was surrounded by liquid nitrogen. Thus it was necessary to introduce helium exchange gas into the calorimeter during the cooling experiment in order to cool the specimen below T_C . Nonetheless, despite these experimental difficulties, we were able to identify the transition temperatures T_N and T_C from these cooling runs.

Comparing the values of the difference ($T_N - T_C$) obtained from warming and cooling experiments, we find that T_C for cooling is about $1.2 \pm 0.4 \text{ K}$ lower than T_C for warming, indicating a temperature hysteresis in the specific heat at T_C . Due to the difficulties mentioned above in performing the cooling experiments, we were not

able to test the dependence of this hysteresis on the rate of change of temperature.

B. Latent heat

The plot of the temperature of the single crystal against time in the region of 91 K during a warming run at constant power input (Fig. 3) is very similar to the equivalent plot (Fig. 2 of Ref. 17) from which the latent heat associated with the discontinuous transition in the terbium single crystal at T_C was estimated. As in the case of terbium, we have assumed that the transition at T_C in dysprosium may be described by the three straight lines shown in Fig. 3. The transition temperature T_C is obtained by the position of the horizontal line and the value $T_C = 91.33 \pm 0.08 \text{ K}$ was obtained for this warming run on the dysprosium single crystal. The length of the straight line gives the time for which the known warming power has been applied to the specimen during the course of the transition. A latent heat of $39.1 \pm 1.5 \text{ J mol}^{-1}$ was determined from the average of those obtained in five warming runs on the single crystal of dysprosium.

A careful examination of Fig. 3 shows that at the Curie point the temperature of the sample rises to a maximum, falls with negative $\partial T/\partial t$, and passes through a minimum before rising again. This phenomenon has been observed much more clearly in our measurements on terbium,^{1,17} and in those papers we attributed it to instrumental effects. However, measurements in which we have made the melting transitions of water and mercury do not show any regions of negative $\partial T/\partial t$. We therefore cannot rule out the possibility that we have observed an intrinsic effect due to superheating of the dysprosium and terbium¹⁷ at the phase transition.

Superheating cannot, of course, occur in an order-disorder transition due to the fact that no process of nucleation is needed to create the disordered phase. However, in an order-order transition, such as that which occurs in terbium and dysprosium, it is necessary to nucleate the high-temperature ordered phase before this phase can grow. Details of the evolution of the helical phase from the ferromagnetic phase in these rare-earth metals via an intermediate-moment bearing domain structure have been discussed in the literature (e.g., Refs. 14 and 18).

One possible explanation of the effect seen in Fig. 3 therefore is that as the temperature rises above the thermodynamic transition temperature, superheating occurs; at the peak in Fig. 3 nucleation and growth of the helical phase starts to take place. In order for growth of the helical phase to occur, latent heat must be made available, and this is done by the reduction of the temperature of the sample as a whole, resulting in the negative values of $\partial T/\partial t$ seen in Fig. 3. The process is therefore a kinetic one, and the details of it, such as the depth of the minimum, will depend on the warming rate and other factors. Further investigation of these effects is warranted.

We have also estimated the latent heat at the Curie temperature of dysprosium from the measurements on the polycrystalline sample. As shown by Fig. 2, the peak in the specific heat at the discontinuous transition at T_C of the polycrystalline sample is not as sharp as that of the

single-crystal sample of Fig. 1. This indicates that the discontinuous transition persists over a wide range of temperature (about 25 K) in the comparatively low-purity polycrystalline dysprosium sample. The latent heat associated with the transition at T_C in the polycrystalline sample can be estimated from the area under the specific-heat curve at T_C , and a value of $35 \pm 5 \text{ J mol}^{-1}$ is estimated as the latent heat of dysprosium. The large error results from the uncertainty in determining the baseline to the curve of the specific heat at T_C of the polycrystalline result. This was primarily due to the unavailability of specific-heat data below 75 K for the polycrystalline sample.

From the earlier dc specific-heat measurement on polycrystalline dysprosium,⁸ a value of $36 \pm 2 \text{ J mol}^{-1}$ for the latent heat has been estimated by McKenna¹⁸ from the area under the peak at T_C . This value is in good agreement with the values of the latent heat estimated from the present single crystal and polycrystalline results. In the Appendix the experimental value of the latent heat is compared with our estimates of the values of the latent heats of both dysprosium and terbium.¹⁷ These estimates have been determined by Clausius-Clapeyron equations using the magnetization and lattice parameter measurements available in the literature.

In summary, we have measured the latent heat associated with the discontinuous transition at the Curie point in the single crystal of dysprosium from a direct calorimetric method for the first time. From the latent heat $L = 39.1 \pm 1.5 \text{ J mol}^{-1}$ we may also obtain the entropy $S = L/T$ associated with the transition. This is $S = (4.28 \pm 0.10) \times 10^{-1} \text{ J mol}^{-1} \text{ K}^{-1}$; as expected this is smaller than the value of $23.0 \text{ J mol}^{-1} \text{ K}^{-1}$ associated with the spin entropy $R \ln(2J + 1)$. From the Boltzmann relation $S = k \ln w$, we find that the number of accessible states (w) is 5.15% higher in the helical state than in the ferromagnetic state. The similar estimate for terbium is 0.74% which is about seven times smaller than the value of 5.15% for dysprosium.

V. CRITICAL PARAMETERS AT THE NÉEL TEMPERATURE

A. Introduction

As for terbium¹ and holmium,² the analysis of the critical specific heat of dysprosium was carried out using the equation of the form

$$C^\pm = (A^\pm / \alpha^\pm) |t|^{-\alpha^\pm} (1 + E^\pm |t|^{x^\pm}) + B^\pm + D^\pm t, \quad (1)$$

where $t = (T - T_N) / T_N$. The positive sign refers to $T > T_N$ and the negative sign refers to $T < T_N$. In this paper the analyses of the critical specific-heat data of the single crystal and the polycrystalline sample of dysprosium are presented. A full discussion of our method of analysis is given in Ref. 1. The critical specific-heat data obtained by Lederman and Salamon¹⁰ on a small single crystal of dysprosium are compared with our data, and an examination of these earlier results is given in Sec. VI.

B. Features of the data in the critical region

1. Data for the single crystal

Figure 4 shows the specific-heat data for the single-crystal dysprosium sample obtained with a warming rate of 1.8 K h^{-1} as a function of $\log_{10} |t|$; the value $T_N = 180.040 \text{ K}$ (as discussed later the value found to be optimum for these data) was used to calculate the appropriate values of $|t|$. Also shown are the curves representing best fits of our data (discussed later) in the regions $-2.4 < \log_{10} |t| < -1.6$ below T_N (between arrows Q and R) and $-2.3 < \log_{10} |t| < -1.1$ above T_N (between arrows S and T) to Eq. (1). The values of the parameters which we used (Table II, column 2) are obtained from the fits discussed in Sec. V E.

As seen in Fig. 4, the data points immediately below T_N for $\log_{10} |t| < -2.4$ ($T > 179.28 \text{ K}$) and the data points immediately above T_N for $\log_{10} |t| < -2.3$ ($T < 180.90 \text{ K}$) do not lie on the fitted curves. As discussed in Sec. II of this paper, instrumental effects may be important in this region. The data points between the arrows R (below T_N) and S (above T_N) in Fig. 4 were not included in the analysis. The data below T_N indicate changes in critical behavior at $\log_{10} |t| = -1.6$ and $\log_{10} |t| = -0.8$ as indicated by arrows Q and P, respectively, in Fig. 4. The data points below T_N for $\log_{10} |t| > -0.8$ ($T < 151.5 \text{ K}$) which are far away from the critical point were not included in the analysis, nor as discussed in Sec. V F are the data in the range $-1.6 < \log_{10} |t| < -0.8$ (between arrows Q and P). The data above T_N between arrows S and T can, unlike the data set between arrows R and P, be represented by Eq. (1) with a single set of parameters.

The following two regions were therefore considered to represent the critical data set, (i) the data below T_N in the region $-2.4 < \log_{10} |t| < -1.6$ (data between the arrows Q and R in Fig. 4), and (ii) the data above T_N in the re-

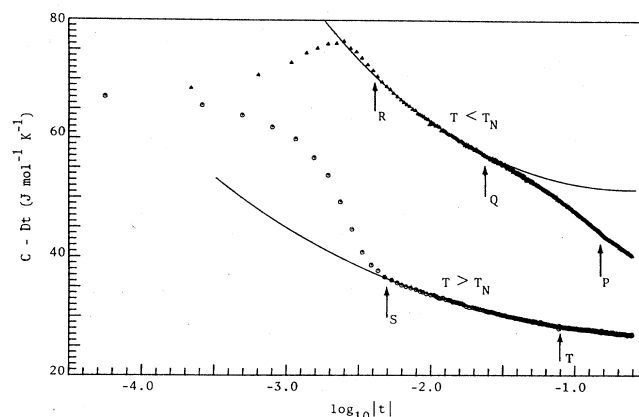


FIG. 4. Specific heat of the dysprosium single crystal around T_N as a function of $\log_{10} |t|$. The value $T_N = 180.040 \text{ K}$ obtained from the fit discussed in Sec. V E is used. Open circles (O) denote the data above T_N and closed triangles (▲) denote data below T_N . The curves are given by the parameters (Table II, column 2) obtained by fitting data in the critical data set to Eq. (1).

gion $-2.3 < \log_{10}|t| < -1.1$ (data between the arrows *S* and *T* in Fig. 4). The analysis of this data set, carried out in terms of the function given in Eq. (1) with and without the confluent singular terms, is discussed in Secs. V E and V D, respectively.

2. Data for the polycrystalline sample

The specific-heat results of the polycrystalline dysprosium sample obtained with a warming rate of 2.1 K h^{-1} are plotted as a function of $\log_{10}|t|$ in Fig. 5; the value $T_N = 180.60 \text{ K}$ determined from the analysis (Sec. V G) was used to calculate the values of $|t|$. Also shown are the best fits of the data to Eq. (1) discussed in Sec. V G (Table IV, column 2).

The data points between arrows *K* (below T_N) and *L* (above T_N) in Fig. 5 are considered to be affected by rounding and were not included in the analysis. The data below T_N for $\log_{10}|t| > -2.0$ cannot be represented by Eq. (1) with a single set of parameters. A careful examination shows a change in behavior at $\log_{10}|t| = -1.5$ (arrow *J* in Fig. 5). The data above T_N for $\log_{10}|t| > -2.3$ can be represented by the function with a single set of parameters up to about $\log_{10}|t| = -1.1$ (arrow *M*). The data below T_N in the region $-2.0 < \log_{10}|t| < -1.5$ (data between arrows *K* and *J* in Fig. 5) and the data above T_N in the region $-2.3 < \log_{10}|t| < -1.1$ (data between arrows *L* and *M* in Fig. 5) were used as the critical data set. The analysis of this data set is discussed in Sec. V G.

C. Constraints on the fitting parameters

As discussed previously,¹ in order to obtain reliable results and to test the overall consistency of theory and the experiment, certain constraints predicted by theory were imposed during this fitting procedure. The constraint $D^+ = D^- = D$ is always imposed in the analysis. A value

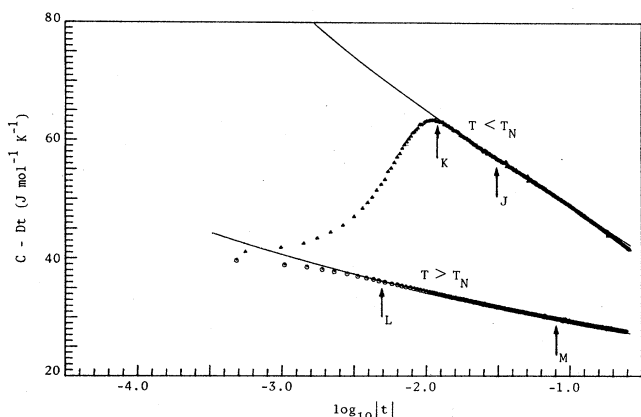


FIG. 5. Specific heat of the dysprosium polycrystalline sample around T_N as a function of $\log_{10}|t|$. The value $T_N = 180.600 \text{ K}$ obtained from the fit discussed in Sec. V G is used. Open circles (O) denote the data above T_N and closed triangles (▲) denote data below T_N . The curves are given by the parameters (Table IV, column 2) obtained by fitting data in the critical data set to Eq. (1).

for D is estimated from the specific heat of nonmagnetic rare-earth metals and the value $D = 4.67 \text{ J mol}^{-1} \text{ K}^{-1}$, determined for the heavy rare-earth metal lutetium¹⁹ at 180 K , was used for the analysis of the dysprosium data. As mentioned in Ref. 1, the critical parameters are not sensitive to the value of D .

D. Pure power-law analysis of the single-crystal data

As for terbium¹ and holmium,² the analysis of dysprosium data was carried out initially using the pure power-law function of the form

$$C^\pm = (A^\pm / \tilde{\alpha}^\pm) |t|^{-\tilde{\alpha}^\pm} + B^\pm + Dt. \quad (2)$$

Adopting a procedure similar to that used for terbium and holmium, we fitted the dysprosium single-crystal data in the critical data set to Eq. (2); the parameters obtained from this pure power-law fit are listed in Table I. These fits showed that the scaling law $\tilde{\alpha}^+ = \tilde{\alpha}^-$ is valid for the dysprosium data in the critical data set; the fit without the constraint $\tilde{\alpha}^+ = \tilde{\alpha}^-$ (Table I, column 2) gave the values $\tilde{\alpha}^+ = 0.34 \pm 0.01$ and $\tilde{\alpha}^- = 0.33 \pm 0.02$. These are consistent with the value $\tilde{\alpha} = 0.33 \pm 0.01$ obtained from the fit with the constraint $\tilde{\alpha}^+ = \tilde{\alpha}^-$ (Table I, column 1). It should be noted that since the regions above and below T_N of the critical data set are relatively far away from the critical point, the pure power-law fit was not very sensitive to the parameter T_N and hence we were not able to test the applicability of the constraint $T_N^+ = T_N^-$ to our dysprosium data. However, since the constraint $T_N^+ = T_N^-$ is valid for terbium¹ and holmium² we have assumed implicitly that it is also valid for our dysprosium data; this

TABLE I. Parameters obtained from the fits of Eq. (2) to the single-crystal data in the critical data set. The data above ($-2.3 < \log_{10}|t| < -1.1$) and below ($-2.4 < \log_{10}|t| < -1.6$) T_N were fitted simultaneously. Column 1: with the constraints $\tilde{\alpha}^+ = \tilde{\alpha}^-$ and $T_N^+ = T_N^-$; column 2: T_N fixed at 179.98 K and $\tilde{\alpha}^+ \neq \tilde{\alpha}^-$; column 3: with the constraints $\tilde{\alpha}^+ = \tilde{\alpha}^-$, $T_N^+ = T_N^-$, and $B^+ = B^-$. The units of A , B , and D are $\text{J mol}^{-1} \text{ K}^{-1}$. The parameter P is defined as $P = (1 - A^+ / A^-) / \tilde{\alpha}$. The errors shown are standard errors. In the present analysis $\sigma_i = 1 \text{ J mol}^{-1} \text{ K}^{-1}$ was used, where σ_i^2 is the variance, which describes the uncertainty of the i th data point (Refs. 1 and 20).

	1	2	3
$\tilde{\alpha}^+$	0.33 ± 0.01^a	0.34 ± 0.01	0.16 ± 0.01^a
$\tilde{\alpha}^-$	0.33 ± 0.01^a	0.33 ± 0.01	0.16 ± 0.01^a
A^+	0.80 ± 0.03	0.80 ± 0.04	1.42 ± 0.02
A^+ / A^-	0.52 ± 0.04	0.53 ± 0.06	0.38 ± 0.01
B^+	22.76 ± 0.24	22.69 ± 0.29	15.07 ± 0.24^b
B^-	41.26 ± 0.61	41.48 ± 1.08	15.07 ± 0.24^b
D	4.67^c	4.67^c	4.67^c
T_N (K)	179.98 ± 0.18	179.98^c	180.16 ± 0.17
χ^2	0.0078	0.0078	0.0250
P	1.52		3.88

^aWith the constraint $\tilde{\alpha}^+ = \tilde{\alpha}^-$.

^bWith the constraint $B^+ = B^-$.

^cFixed.

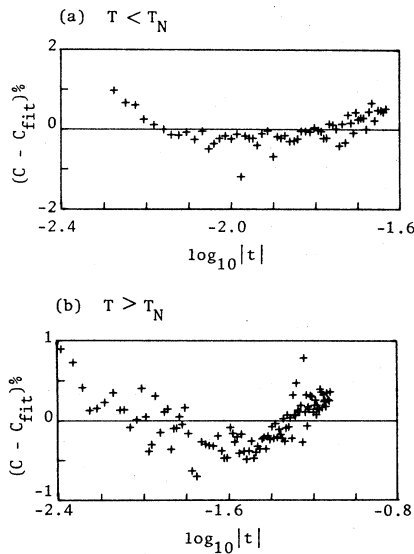


FIG. 6. Deviations of the experimental specific-heat data of the single crystal from the fit (Table I, column 3) obtained by fitting data in the critical data set to Eq. (2) with the constraint $B^+ = B^-$: (a) for data below T_N and (b) for data above T_N ($T_N = 180.160$ K).

assumption would appear to be justified by the regularities of the scatter diagrams that we obtain (Figs. 8 and 10).

As for terbium¹ and holmium,² the parameters listed in Table I, column 3 indicate that the constraint $B^+ = B^-$ is unacceptable for the analysis of the dysprosium data using a pure power-law function because (a) as shown in Fig. 6, the scatter diagrams obtained from the parameters of the fit with the constraint $B^+ = B^-$ show systematic deviations from the fits, and (b) the value of χ^2 obtained for the fit with the constraint $B^+ = B^-$ is significantly higher (about three times) than that obtained for the fit without the constraint $B^+ = B^-$. Therefore, in order to test whether the inclusion of confluent singular terms in the function will permit the values of B^+ and B^- to be the same, we fitted the dysprosium single-crystal data in the critical data set to Eq. (1); the results of this analysis are presented in Sec. V E.

The pure power-law analysis (e.g., Table I, column 1) was carried out on data of two more runs with warming rates 2.8 and 3.4 K h⁻¹. Figure 7(a) shows the values of T_N determined from the pure power-law analysis as a function of warming rate. This shows that the value of the intrinsic Néel temperature of the dysprosium single crystal is 179.90 ± 0.18 K and is independent of rate within the error indicated. The effective critical exponents $\tilde{\alpha}$ obtained from the pure power-law analyses (e.g., Table I, column 1) of three experimental runs are plotted against the warming rate in Fig. 7(b). The scatter is consistent with a value of $\tilde{\alpha} = 0.33 \pm 0.02$.

E. Analysis with confluent terms—single-crystal data

As for terbium¹ and holmium,² the single-crystal data in the critical data set were fitted to Eq. (1) while retain-

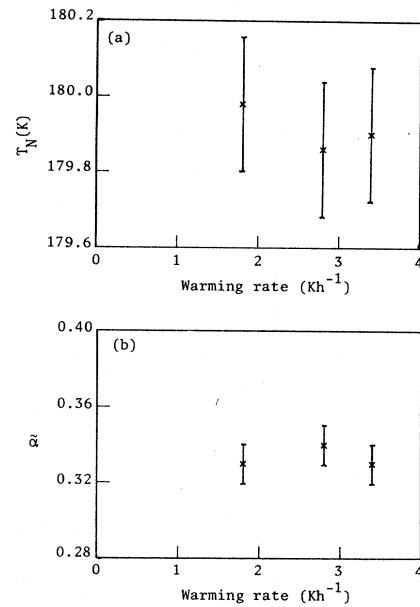


FIG. 7. (a) Transition temperature T_N of the single crystal obtained from the fits to Eq. (2), plotted against the warming rate as measured at 150 K. The intrinsic Néel temperature of the dysprosium single crystal is 179.90 ± 0.18 K. (b) The effective critical exponent $\tilde{\alpha}$ determined from all the experimental results as a function of warming rate. The scatter is consistent with a value of $\tilde{\alpha} = 0.33 \pm 0.02$.

ing the constraints $\alpha^+ = \alpha^-$ and $T_N^+ = T_N^-$ and the fixed values of $D = 4.67$ J mol⁻¹ K⁻¹ and $x^+ = x^- = 0.5$ (see Refs. 1 and 2); the parameters obtained are listed in Table II. The parameters of the fit without the constraint $B^+ = B^-$ (Table II, column 1) indicate that the values of B^+ and B^- differ by 91 J mol⁻¹ K⁻¹ and the value of B^- has the very high value of 129.86 J mol⁻¹ K⁻¹. However, the results of the fit with the constraint $B^+ = B^-$ (Table II, column 2) indicate that the value $B^+ = B^-$ is 16.49 J mol⁻¹ K⁻¹, which is of the order of the value of the specific heat of lutetium¹⁹ at 180 K (25 J mol⁻¹ K⁻¹). If the fit with the constraint $B^+ = B^-$ (Table II, column 2) is considered to be the optimum fit to our dysprosium data, and if the latter value can be taken to represent the background specific heat of dysprosium, this would imply that for dysprosium the part of B associated with critical effects has a small negative value of -8.5 ± 1.5 J mol⁻¹ K⁻¹. For terbium¹ the part of B associated with critical effects has a value close to zero (-4.4 ± 13.9 J mol⁻¹ K⁻¹). Furthermore, the value of $\alpha = 0.24 \pm 0.02$ obtained for dysprosium with the constraint $B^+ = B^-$ is close to the value $\alpha = 0.20 \pm 0.03$ obtained for terbium.¹ Because of this agreement of our results for dysprosium listed in Table II, column 2 with comparable results of terbium,¹ and also because the value of $P = 2.46$ determined from the fit with the constraint $B^+ = B^-$ (Table II, column 2) lies within the range of values found in other materials (see Refs. 1 and 21), we consider that the parameters listed in Table II, column 2 represent the optimum fit to our dysprosium critical data,

TABLE II. Parameters obtained from the fits of Eq. (1) to the single-crystal data in the critical data set. The data above $(-2.3 < \log_{10}|t| < -1.1)$ and below $(-2.4 < \log_{10}|t| < -1.6)T_N$ were fitted simultaneously. Column 1: with the constraints $\alpha^+ = \alpha^-$ and $T_N^+ = T_N^-$; column 2: with the constraints $\alpha^+ = \alpha^-$, $T_N^+ = T_N^-$, and $B^+ = B^-$. The units of A , B , and D are $\text{J mol}^{-1} \text{K}^{-1}$. The errors shown are standard errors.

	1	2
α^+	0.46 ± 0.02^a	0.24 ± 0.02^a
α^-	0.46 ± 0.02^a	0.24 ± 0.02^a
A^+	0.42 ± 0.06	1.27 ± 0.11
A^+/A^-	0.96 ± 0.07	0.41 ± 0.05
B^+	38.80 ± 2.42	16.49 ± 1.50^b
B^-	129.86 ± 5.26	16.49 ± 1.50^b
E^+	-16.26 ± 1.01	0.77 ± 0.13
E^+/E^-	0.17 ± 0.23	0.41 ± 0.18
D	4.67^c	4.67^c
x	0.5^c	0.5^c
T_N (K)	179.88 ± 0.19	180.04 ± 0.18
χ^2	0.0077	0.0088
P	0.09	2.46

^aWith the constraint $\alpha^+ = \alpha^-$.

^bWith the constraint $B^+ = B^-$.

^cFixed.

even though the fit with the constraint $B^+ = B^-$ is no better in χ^2 than the fit without this constraint (Table II, column 1), The scatter diagrams shown in Fig. 8 were obtained from the parameters listed in Table II, column 2; the random scatter of the deviations of the data points from the fitted curves indicate that the data are represented well by the parameters obtained from the fit.

The experimental points around the Néel temperature are plotted as a function of temperature on a linear scale in Fig. 9(a). Also shown are the fitted curves obtained

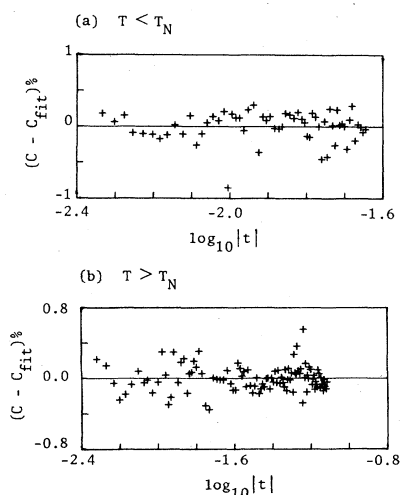


FIG. 8. Deviations of the experimental specific-heat data for the single crystal from the fit (Table II, column 2) obtained by fitting data in the critical data set to Eq. (1): (a) for data below T_N and (b) for data above T_N ($T_N = 180.040$ K).

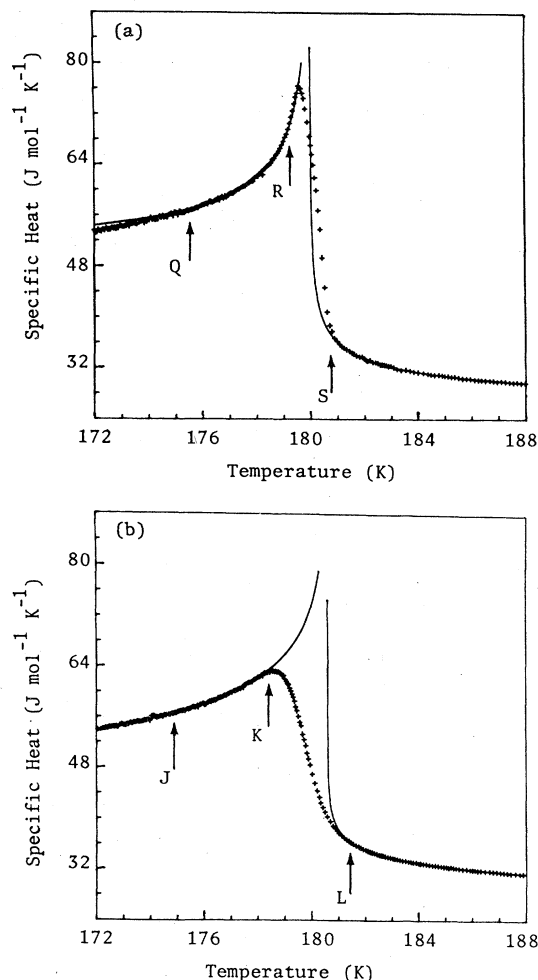


FIG. 9. (a) Experimental data points for the dysprosium single crystal near the Néel temperature plotted against temperature. The lines through the points are the fitted curves obtained from the parameters given in Table II, column 2. Data for temperatures between the arrows R and S are not part of the critical data set. (b) Experimental data points for the polycrystalline dysprosium sample near the Néel temperature plotted against temperature. The lines through the points are the fitted curves obtained from the parameters given in Table IV, column 2. Data for temperatures between the arrows K and L are not part of the critical data set.

from the parameters of Table II, column 2. It should be noted that the data above T_N for $\log_{10}|t| < -2.3$ ($T < 180.90$ K) lie above the fitted curve [Figs. 4 and 9(a)]. This is not consistent with effects of impurities in the sample, which in our view should produce data points which all lie below the fitted curve as is the case for the polycrystalline sample, shown in Fig. 9(b). The change in behavior of the data observed above T_N at $\log_{10}|t| = -2.3$ could of course be due to a genuine crossover such as we observed in terbium¹ and holmium.² A close inspection of data reveals that only five points immediately below $\log_{10}|t| = -2.3$ [i.e., immediately below the arrow S in Figs. 4 and 9(a)] behave in a manner con-

sistent with the behavior of terbium and holmium, and that the other data points above T_N for $\log_{10}|t| < -2.7$ do indeed suggest rounding. As there are only five data points immediately below the arrow S , it is not reasonable to fit them to our function. Further, as mentioned earlier (Sec. II), because of the small size of the dysprosium single crystal, the specific-heat data may not be accurate close to the transition. Therefore, we are unable to comment further regarding the behavior of the data of the dysprosium single crystal in the region between points R and S .

F. Single-crystal data below T_N for $\log_{10}|t| > -1.7$

As mentioned before, the data for the single crystal below T_N exhibit a change in behavior at $\log_{10}|t| = -1.6$ (Fig. 4). The critical exponent α obtained for data below T_N for $\log_{10}|t| < -1.6$ is positive, as demonstrated by the concave-upward curvature of the data in Fig. 4. As can also be seen in Fig. 4, the data below T_N for $\log_{10}|t| > -1.6$ between arrows Q and P indicate that the value of the critical exponent α is negative. However, by fitting the data set below T_N for $\log_{10}|t| > -1.6$ to the function given in Eq. (1), we were not able to obtain sensible values for the parameters; the parameters obtained were unphysical, such as $B^- = -160 \text{ J mol}^{-1} \text{ K}^1$ and $\tilde{\alpha}^- = +0.02$. Since these data points below T_N lie relatively far away from the critical point [arrow Q in Fig. 9(a); $T = 175.52 \text{ K}$], we cannot attach a great deal of significance to them.

G. Analysis of the polycrystalline sample data

As with the single-crystal data, the analysis of the data in the critical data set of the polycrystalline sample was carried out in terms of the function given in Eq. (1). First, the analysis was performed with the pure power-law function [Eq. (2)]; the results obtained are listed in Table III. These fits showed that the scaling law $\tilde{\alpha}^+ = \tilde{\alpha}^-$ is

TABLE III. Parameters obtained from the fits of Eq. (2) to the polycrystalline sample data in the critical data set. The data above $(-2.3 < \log_{10}|t| < -1.1)$ and below $(-2.0 < \log_{10}|t| < -1.5)T_N$ were fitted simultaneously. Column 1: with the constraints $\tilde{\alpha}^+ = \tilde{\alpha}^-$ and $T_N^+ = T_N^-$; column 2: T_N fixed at 180.50 K and $\tilde{\alpha}^+ \neq \tilde{\alpha}^-$; column 3: T_N fixed at 180.20 K and $\tilde{\alpha}^+ = \tilde{\alpha}^-$. The units of A , B , and D are $\text{J mol}^{-1} \text{ K}^{-1}$.

	1	2	3
$\tilde{\alpha}^+$	0.09 ± 0.04^a	0.09 ± 0.04	0.15 ± 0.04^a
$\tilde{\alpha}^-$	0.09 ± 0.04^a	0.07 ± 0.05	0.15 ± 0.04^a
A^+	1.65 ± 0.19	1.69 ± 0.20	1.47 ± 0.16
A^+/A^-	0.34 ± 0.06	0.32 ± 0.08	0.42 ± 0.05
B^+	8.40 ± 0.84	5.39 ± 0.95	15.37 ± 1.03
B^-	-15.26 ± 1.52	-40.99 ± 2.41	16.66 ± 1.42
D	4.67^b	4.67^b	4.67^b
T_N (K)	180.50 ± 0.32	180.50^b	180.20^b
χ^2	0.0042	0.0042	0.0053
P	7.33		3.87

^aWith the constraint $\tilde{\alpha}^+ = \tilde{\alpha}^-$.

^bFixed.

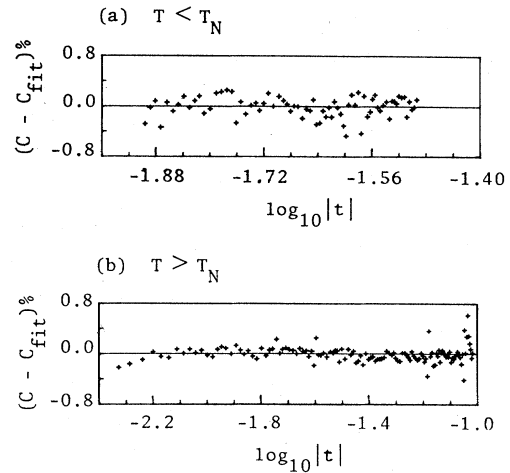


FIG. 10. Deviations of the experimental specific-heat data of the polycrystalline sample from the fit (Table IV, column 2) obtained by fitting data in the critical data set to Eq. (1): (a) for data below T_N and (b) for data above T_N ($T_N = 180.60 \text{ K}$).

valid for the data in the critical data set (see columns 1 and 2 of Table III). However, as with the single-crystal data, we were not able to test the applicability of the constraint $T_N^+ = T_N^-$ to our polycrystalline data and we have assumed that the constraint $T_N^+ = T_N^-$ is also valid for our polycrystalline data. The scatter diagrams in Fig. 10 suggest that this assumption is valid.

As can be seen in Table III, column 1, the pure power-law fit indicates that the value of B^- is negative and $B^+ \neq B^-$. However, the parameters of the pure power-law fit with a fixed value of $T_N = 180.200 \text{ K}$, listed in Table III, column 3 indicate that the values of B^+ and B^- are the same within about 8% but at the expense of a slightly worse χ^2 . Also note that the value of $\tilde{\alpha}$ obtained for the polycrystalline data is 0.09 ± 0.04 whereas that obtained for the single-crystal data is 0.33 ± 0.01 . According to the criterion of Harris²¹ the presence of impurities in the sample would contribute to the rounding, however, an estimate shows that this should be insignificant. The specific-heat measurements of Williams *et al.*²² on gadolinium showed that strain effects can both shift the temperature of the peak and also the values of the absolute specific heat (see Fig. 2 of Ref. 22). Therefore, the possibility exists that, besides the rounding effects, the critical behavior around the critical point could also be changed due to inhomogeneities in the sample.²³ As mentioned before, the critical behavior near T_N of the polycrystalline dysprosium sample has been affected severely by rounding, and this could be the reason why the critical exponent α obtained from analysis of the polycrystalline sample data is different to that obtained from the single-crystal data.

We have also fitted the dysprosium polycrystalline data in the critical data set to Eq. (1) while retaining the constraints $\alpha^+ = \alpha^-$ and $T_N^+ = T_N^-$ and the fixed values of $D = 4.67 \text{ J mol}^{-1} \text{ K}^{-1}$ and $x^+ = x^- = 0.5$; the parameters obtained are listed in Table IV. The deviations of the data

points in the critical data set from the fitted curves estimated from the parameters of Table IV, column 2 are shown in Fig. 10. The other fits listed in Table IV, column 1 and Table III also exhibited very similar scatter diagrams. The values of the parameters obtained with the constraint $B^+ = B^-$ (Table IV, column 2) are not greatly different to those obtained for the single-crystal data from the similar fit (Table II, column 2). Furthermore, the value of $P = 4.86$ lies within the range of values found from theoretical estimates and also in other materials (see Refs. 1 and 21). Therefore, we consider that the parameters listed in Table IV, column 2 represent the optimum fit[Ⓢ] to the critical data of our polycrystalline sample.

The experimental data points for the polycrystalline dysprosium sample are plotted against temperature on a linear scale in Fig. 9(b) together with the fitted curves estimated from the parameters of Table IV, column 2. As can be seen, the critical data for the polycrystalline sample have been substantially affected by rounding which has also shifted the peak temperature of the specific heat down by about 2 K.

H. Summary

We have analyzed the critical specific heat of the dysprosium single crystal and the polycrystalline sample in terms of the function given in Eq. (1). The analysis was performed with and without the inclusion of confluent singular terms. The results obtained for the single crystal are listed in Tables I and II, and those obtained for the polycrystalline sample are listed in Tables III and IV. Our analysis showed that the scaling law $\alpha^+ = \alpha^-$ is valid for the critical data of dysprosium. The parameters of the fit for the single crystal that we regard as most satisfacto-

TABLE IV. Parameters obtained from the fits of Eq. (1) to the polycrystalline sample data in the critical data set. The data above $(-2.3 < \log_{10}|t| < -1.1)$ and below $(-2.0 < \log_{10}|t| < -1.5)T_N$ were fitted simultaneously. Column 1: with the constraints $\alpha^+ = \alpha^-$ and $T_N^+ = T_N^-$; column 2: with the constraints $\alpha^+ = \alpha^-$, $T_N^+ = T_N^-$, and $B^+ = B^-$. The units of A , B , and D are $\text{J mol}^{-1} \text{K}^{-1}$.

	1	2
α^+	0.09 ± 0.04^a	0.14 ± 0.05^a
α^-	0.09 ± 0.04^a	0.14 ± 0.05^a
A^+	1.61 ± 0.24	1.11 ± 0.09
A^+/A^-	0.37 ± 0.04	0.32 ± 0.03
B^+	8.31 ± 1.01	20.13 ± 4.32^b
B^-	-5.32 ± 0.91	20.13 ± 4.32^b
E^+	-0.02 ± 0.52	-0.49 ± 1.02
E^+/E^-	0.13 ± 3.23	0.97 ± 2.26
x	0.5^c	0.5^c
D	4.67^c	4.67^c
T_N (K)	180.50 ± 0.37	180.60 ± 0.41
χ^2	0.0042	0.0043
P	7.00	4.86

^aWith the constraint $\alpha^+ = \alpha^-$.

^bWith the constraint $B^+ = B^-$.

^cFixed.

ry are listed in Table II, column 2, whereas our optimum parameters for the polycrystalline sample are listed in Table IV, column 2. Our optimum parameters for the polycrystalline sample (Table IV, column 2) are not substantially different (not more than two standard errors) to those for the single crystal (Table II, column 2). The inclusion of confluent singular terms in the function, although it did not significantly alter the value of χ^2 , made possible the imposition of the constraint $B^+ = B^-$ in the analysis of data.

VI. PREVIOUS RESULTS OBTAINED FOR DYSPROSIUM

As discussed above, rounding effects have obscured the behavior of the critical data close to the critical point of the dysprosium samples of the present study. Lederman and Salamon¹⁰ reported that their data on a small single crystal in the critical region up to $\log_{10}|t| = -3.3$ on both sides of T_N could be used for analysis, and that only the data immediately below and above T_N for $\log_{10}|t| < -3.3$ had been affected by rounding. We have examined the earlier results of Lederman and Salamon¹⁰ for dysprosium in detail and have found that some of the fitting parameters given by them for the data in the region $-3.3 < \log_{10}|t| < -2.3$ are in error. The fitted curves derived by us using the values of parameters given by Lederman and Salamon¹⁰ for their "inner region," $-3.3 < \log_{10}|t| < -2.3$, differ considerably from the experimental data.²⁴

For comparison, the present results from our single

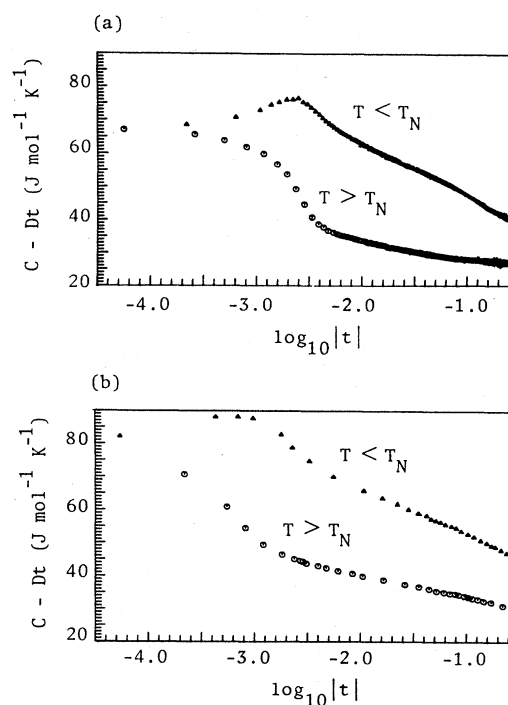


FIG. 11. Specific heat of the single crystal of dysprosium as a function of $\log_{10}|t|$. (a) Results of the present study ($T_N = 180.040 \text{ K}$). (b) Results of Lederman and Salamon (Ref. 10) ($T_N = 183.15 \text{ K}$).

crystal of dysprosium and the results of Lederman and Salamon¹⁰ for their single crystal of dysprosium are plotted on the same scales in Fig. 11(a) and 11(b), respectively. Although there are differences in the absolute values of the two sets of results, the general behavior of the critical data of both sets is essentially similar. However, it should be noted that rounding effects have obscured the critical data close to T_N in our present results [Fig. 11(a)] thus making it difficult to make a detailed comparison of our results with those of Lederman and Salamon.¹⁰

As discussed previously,¹ the method of analysis used by Lederman and Salamon¹⁰ has led them to assume that a crossover takes place at the same value of $|t|$ above and below T_N , which is not necessarily the case. This in turn has led them to deduce possibly incorrect values for the critical parameters. We consider that their claim of a crossover at $\log_{10}|t| = -2.3$ on both sides of T_N of dysprosium is incorrect. We observed a similar false indication of a crossover in the terbium data below T_N when we used the method of Salamon²⁵ to analyze the data for our terbium single crystal.¹ In conclusion we find that shortcomings in the analysis of the earlier critical data on dysprosium¹⁰ do not allow a useful comparison to be made with our results.

VII. DISCUSSION

During this study we have measured the specific heat of a small high-purity (99.6 at. %) single crystal and a larger relatively impure (92 at. %) polycrystalline sample of dysprosium. The appearance of a sharp peak at T_C and a much sharper peak at T_N of the dysprosium single crystal (Fig. 1), compared with the result of the present dysprosium polycrystalline sample (Fig. 2) and the earlier result of Griffel *et al.*,⁸ reflects the higher purity of our single-crystal dysprosium sample. However, as discussed earlier, considerable rounding of the transition at T_N was observed in both the single crystal and the polycrystalline sample results; these rounding effects are considered to be associated with inhomogeneities in the case of the polycrystalline specimen and instrumental effects for the single crystal.

The Néel temperature T_N of the dysprosium single crystal is 179.90 ± 0.18 K and no dependence of T_N on warming rate was observed. This value is in good agreement with the value of 179.5 ± 0.3 K obtained for the same single crystal from ac susceptibility measurements.²⁶ This agreement is expected in view of the continuous nature of the transition. By comparison, the T_C values from specific heat and ac magnetic susceptibility measurements are 91.33 ± 0.08 K (Fig. 3) and 89.0 ± 0.3 K (Ref. 26) respectively. This difference between the values of T_C for the single crystal could be due to the influence of the temperature at which the experiment was first started²⁷ and hysteretic effects²⁷ at the discontinuous transition. Similar behavior is found for the polycrystalline sample.

A. Transition from ferromagnetism to helical antiferromagnetism

The present study provides conclusive evidence for the discontinuous nature of the ferromagnetic-anti-

ferromagnetic transition in dysprosium at T_C . The sharp peak observed in the specific heat of the single crystal result (Fig. 1) and the plateaulike behavior observed at T_C in the plot of the specimen temperature against time (Fig. 3) demonstrate that the transition is discontinuous. The value obtained for the latent heat at T_C of the single-crystal dysprosium sample is 39.1 ± 1.5 J mol⁻¹ and, as mentioned before, this is the first direct calorimetric measurement of this quantity. We have also estimated the latent heat at T_C of the polycrystalline dysprosium sample, and a value of 35 ± 5 J mol⁻¹ was obtained in good agreement with the value of the single-crystal sample. A further indication of the discontinuous nature of this transition is the existence of a temperature hysteresis at T_C . For the single-crystal dysprosium sample we observed a temperature hysteresis of 1.2 ± 0.4 K in the specific heat at T_C . This is in excellent agreement with the value 1.2 ± 0.1 K reported for the temperature hysteresis in ac susceptibility measurements of the same single crystal.²⁶ However, we were not able to estimate a value for the temperature hysteresis in the specific heat of the polycrystalline dysprosium sample due to the difficulties in performing extended cooling experiments (see Sec. IV A).

B. Critical specific heat of dysprosium

1. Introduction

Since the magnetic behavior of dysprosium in the critical region is similar to that of terbium, much of the information presented by Jayasuriya *et al.*¹ concerning magnetic interactions in terbium is also relevant to the discussion of dysprosium, and in the interest of brevity will not be repeated here. No predictions of the critical parameters are at present available for incommensurate xy systems ($d=3$, $n=2$).

2. Previous results for α

An estimate of the critical exponent α for dysprosium has been obtained from the analyses of specific heat¹² and resistivity²⁸ data of dysprosium specimens. Amitin and co-workers^{12,28} claim that the scaling law $\alpha^+ = \alpha^-$ and the condition $T_N^+ = T_N^-$ are invalid for the critical region of dysprosium. They fitted the data above and below T_N separately to a power-law function and obtained positive values for α^+ (+0.12 to +0.49) and negative values for α^- (-0.205 to -0.25) from both the resistivity and specific-heat data. Furthermore, the values of T_N^+ (or T_N^-) determined from different data sets above T_N (or below T_N) are different; e.g., the values of T_N^+ obtained from the specific-heat data above T_N in the regions $-2.0 < \log_{10}|t| < -0.9$ and $-1.3 < \log_{10}|t| < -0.4$ are 180.9 and 178 K, respectively.¹² The results of the analyses of these workers are in disagreement with our results.

An estimate of the specific-heat critical exponent α for dysprosium has also been obtained by Balberg and Maman²⁹ and Malmstrom and Geldart³⁰ from an analysis of the critical resistivity data of Rao *et al.*,³¹ assuming that the critical behavior of $\partial\rho/\partial T$ is similar to that of the specific heat. Balberg and Maman²⁹ obtained the value

$\alpha^+ = \alpha^- = -0.04 \pm 0.005$ for the resistivity data in the regions $-3.5 < \log_{10} |t| < -1.52$ above and below T_N . However, Malmstrom and Geldart³⁰ obtained the value $\alpha^+ = \alpha^- = -0.20 \pm 0.05$ for the same resistivity data in the regions $-4.4 < \log_{10} |t| < -1.7$ above and below T_N . Malmstrom and Geldart³⁰ claimed that $\alpha = -0.20 \pm 0.05$ is the correct value for dysprosium because their value is in agreement with the value $\alpha = -0.17$ derived from theory for the $n=4$ system which describes (according to Droz and Coutinho-Filho³² and Bak and Mukamel³³) the behavior of the transition from paramagnetism to planar-helical order. The disagreement between these two analyses of the same resistivity data of Rao *et al.*³¹ is clear. The assumption of similar critical behavior of the temperature derivative of the resistivity and the specific heat may also not be valid. The value of the specific-heat critical exponent α obtained from the present specific-heat results on the single crystal is $+0.24 \pm 0.02$ for both the region $-2.4 < \log_{10} |t| < -1.6$ below T_N and the region $-2.3 < \log_{10} |t| < -1.1$ above T_N , in disagreement with any of the results obtained from resistivity data. As can be seen from the concave-upward curvature of the data in Fig. 4, the value of α is definitely positive for the regions mentioned above. We note that we have also observed positive values of α for the magnetically similar systems terbium¹ and holmium.²

3. Conclusion

Our best estimate of the critical exponent α for the single crystal of dysprosium is 0.24 ± 0.02 (Table II, column 2) and that for the polycrystalline sample, taken over a similar region of $|t|$, is 0.14 ± 0.05 , a value not greatly different to the value for the single crystal. The analyses of the data on both the single crystal and the polycrystalline sample demonstrate that the scaling law $\alpha^+ = \alpha^-$ is valid for the dysprosium data. We also found that in order to obtain the condition $B^+ = B^-$ it is necessary to include confluent terms in the fitting function.

As for the cases of terbium¹ and holmium,² the value of the exponent α (0.24 ± 0.02) found from this study of dysprosium does not agree with the $n=2$ prediction (-0.02) for short-range exchange systems and the $n=4$ prediction (-0.17) of Droz and Coutinho-Filho³² and Bak and Mukamel.³³ However, the value of $\alpha = 0.24 \pm 0.02$ obtained for dysprosium is reasonably close to the value of $\alpha = 0.20 \pm 0.03$ obtained for terbium¹ and also to the value of $\alpha = 0.27 \pm 0.02$ obtained for holmium.² As for holmium, the values of A^+/A^- , E^+/E^- , and P are not in agreement with any of the classical renormalization-group predictions; however, the values of P do lie within the range of values found for other materials (see Refs. 1 and 21). The predictions of critical parameters for $d=3$, $n=2$ incommensurate systems are not available for us to make a comparison of them with our results.

Calculations which take the competing effects of nearest- and next-nearest-neighbor interactions into account have indicated that the critical behavior of incommensurate systems could depend on the value of $k = -J_2/J_1$, where $-J_2$ and J_1 are the coupling con-

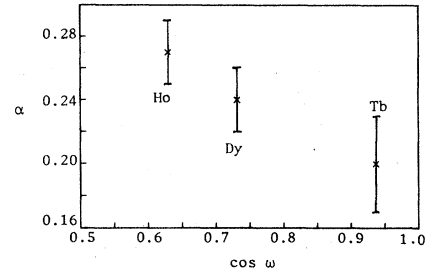


FIG. 12. Critical exponents α for terbium (Ref. 1), dysprosium (present study), and holmium (Ref. 2) plotted as a function of $\cos \omega$, where ω is the turn angle of the helical ordering.

stants of the next-nearest- and nearest-neighbor interactions, respectively.³⁴ These coupling constants are related to the spiral turn angle ω by the relation $\cos \omega = -J_1/4J_2$. The values of α for terbium, dysprosium, and holmium are plotted as a function of $\cos \omega$ in Fig. 12; this figure indicates that the critical exponent α for incommensurate systems, such as those of the rare earths may exhibit a slight dependence on ω , thereby demonstrating a possible nonuniversal behavior. According to Barber,³⁵ the critical exponents for $d=2$ incommensurate systems may be nonuniversal; it is not known whether this is true for $d=3$ systems. However, as discussed above, our results on terbium, dysprosium, and holmium tend to suggest that this might be the case.

ACKNOWLEDGMENTS

We thank members of the Department of Physics of the University of New South Wales, Faculty of Military Studies, Duntroon for the loan of the dysprosium specimens.

APPENDIX: ESTIMATES OF THE LATENT HEAT

In this appendix the values of the latent heat associated with the discontinuous transitions in terbium and dysprosium at the Curie temperature T_C are estimated from the available measurements of the magnetization and of the lattice parameters for terbium and dysprosium that are reported in the literature.

The Gibbs function (per unit volume) can be defined³⁶ as

$$g = u - Ts - \mathbf{H} \cdot \mathbf{m} + \vec{\sigma} \cdot \vec{\epsilon}, \quad (\text{A1})$$

where u is the internal energy, s is the entropy \mathbf{m} the magnetization, \mathbf{H} the magnetic field, $\vec{\sigma}$ the stress, and $\vec{\epsilon}$ the strain. Equation (A1) leads, together with the fundamental thermodynamic relation $du = Tds + \mathbf{H} \cdot d\mathbf{m} - \vec{\sigma} \cdot d\vec{\epsilon}$, to

$$dg = -sdT - \mathbf{m} \cdot d\mathbf{H} + \vec{\epsilon} \cdot d\vec{\sigma}, \quad (\text{A2})$$

where

$$\vec{\epsilon} \cdot d\vec{\sigma} = \sum_{i,j} \epsilon^{ij} d\sigma^{ij}. \quad (\text{A3})$$

The general thermodynamic condition for phase equilibri-

TABLE V. Our estimates of the latent heats L of terbium and dysprosium obtained from magnetization results of various authors. The experimental values of L for terbium and dysprosium are also shown.

	Measurement	L (J mol ⁻¹)	Reference
Tb	Specific heat	13.6±0.6	Jayasuriya <i>et al.</i> (Ref. 17)
	Magnetization	11 ±5	Hegland <i>et al.</i> (Ref. 40)
	Magnetization	15 ±5	Feron (Ref. 38)
	Magnetization	17 ±3	Greenough and Hettiarachchi (Ref. 41)
Dy	Specific heat	39.1±1.5	Present study
	Magnetization	48 ±6	Behrendt <i>et al.</i> (Ref. 37)
	Magnetization	55 ±8	Feron (Ref. 38)
	Magnetization	57 ±6	Fort <i>et al.</i> (Ref. 39)

um is the equality of the Gibbs function g of the two phases, i.e.,

$$g_1 = g_2. \quad (\text{A4})$$

The suffix 1 denotes the phase which is stable on the low-temperature side of the equilibrium. Thus

$$dg_1 = dg_2, \quad (\text{A5})$$

under changes of T , \mathbf{H} , or $\vec{\sigma}$. Therefore, Eqs. (A2) and (A5) lead to

$$-s_1 dT - \mathbf{m}_1 \cdot d\mathbf{H} + \vec{\epsilon}_1 \cdot d\vec{\sigma} = -s_2 dT - \mathbf{m}_2 \cdot d\mathbf{H} + \vec{\epsilon}_2 \cdot d\vec{\sigma}, \quad (\text{A6})$$

i.e.,

$$(s_2 - s_1)dT + (\mathbf{m}_2 - \mathbf{m}_1) \cdot d\mathbf{H} - (\vec{\epsilon}_1 - \vec{\epsilon}_2) \cdot d\vec{\sigma} = 0. \quad (\text{A7})$$

For a system with orthorhombic or higher symmetry

$$\epsilon^{ij} = \delta^{ij} \epsilon^{ii}, \quad (\text{A8})$$

where

$$\delta^{ij} = \begin{cases} 1 & \text{if } i = j \\ 0 & \text{otherwise.} \end{cases}$$

Therefore, Eq. (A7) can be written as

$$\Delta s dT + \sum_{\alpha} \Delta m^{\alpha} dH^{\alpha} - \sum_i \Delta \epsilon^{ii} d\sigma^{ii} = 0, \quad (\text{A9})$$

where $\Delta s = s_1 - s_2$, $\Delta m = m_2 - m_1$, and $\Delta \epsilon = \epsilon_2 - \epsilon_1$. Taking partial derivatives of Eq. (A9), we have

$$\Delta s = -\Delta m^{\alpha} \left[\frac{\partial H^{\alpha}}{\partial T} \right]_{\sigma^{ii}}, \quad (\text{A10})$$

and

$$\Delta s = \Delta \epsilon^{ii} \left[\frac{\partial \sigma^{ii}}{\partial T} \right]_{H^{\alpha}}. \quad (\text{A11})$$

Under hydrostatic pressure, p , we have

$$\sigma^{ij} = p \delta^{ij} \quad \text{and} \quad \Delta v = \sum_i \epsilon^{ii},$$

and we obtain

$$\Delta s = \sum_i \epsilon^{ii} \left[\frac{\partial p}{\partial T} \right] = \Delta v \left[\frac{\partial p}{\partial T} \right], \quad (\text{A12})$$

which is the standard Clausius-Clapeyron equation, where Δv is the change in volume at T_C .

For dysprosium, isothermal magnetization data have been reported by Behrendt *et al.*,³⁷ Feron,³⁸ and Fort *et al.*³⁹ for applied fields along the a axis (the easy axis of magnetization). Using these magnetization data and Eq. (A10), we have estimated the values for the latent heat ($L = \Delta s T_C$) at T_C of dysprosium, and these estimates are summarized in Table V. For terbium, isothermal magnetization data for applied fields along the b axis (the easy axis of magnetization) have been reported by Hegland *et al.*⁴⁰ and Greenough and Hettiarachchi,⁴¹ and those for applied fields along the a axis have been obtained by Feron.³⁸ Using these magnetization data we have estimated¹⁷ the values of the latent heat using Eq. (A10), and

TABLE VI. Variation with uniaxial stress (Ref. 42) and hydrostatic pressure (Ref. 43) of the temperature of the transitions from ferromagnetism to helical antiferromagnetism of terbium and dysprosium.

	T_C (K)	$\partial T_C / \partial \sigma^{cc}$ (K/kbar)	$\partial T_C / \partial \sigma^{aa}$ (K/kbar)	$\partial T_C / \partial \sigma^{bb}$ (K/kbar)	$\partial T_C / \partial p$ (K/kbar)
Tb	220.8	-2.4±0.1	5.7±0.5	5.7±0.5	-1.24±0.02
Dy	89.9	-10.8±0.5	1.7±0.1	9.9±0.5	-1.27±0.02

TABLE VII. Discontinuous changes in the lattice parameters of terbium and dysprosium at T_C .

	Reference	$10^3(c_2-c_1)/c$	$10^3(a_2-a_1)/a$	$10^3(b_2-b_1)/b$	$10^3(v_2-v_1)/v$
Tb	Finkel <i>et al.</i> (Ref. 45)	-0.19			-0.168
Tb	White (Ref. 46)			+0.1	
Dy	Darnell and Moore (Ref. 47)	-1.91	-2.37	4.59	-0.268
Dy	Finkel and Vorobev (Ref. 48)	-1.49	5.90	-1.43	+2.93

these estimates are also summarized in Table V. Our estimates of the latent heat for terbium from magnetization data are in agreement with the value measured directly during this study within experimental error. All our estimates of L for dysprosium from the magnetization data of various authors have higher values than the value measured during this study (see Table V).

For terbium and dysprosium the effects of uniaxial stress on the magnetic transition temperatures have been determined by Bartholin *et al.*⁴² for spherical specimens, and the effects of hydrostatic pressure on the magnetic transition temperatures have been determined by Bartholin and Bloch.⁴³ The variations with uniaxial stress and hydrostatic pressure of the ferromagnetic-helical-antiferromagnetic transition temperatures of terbium and dysprosium^{42,43} are given in Table VI.

The lattice parameter measurements of Darnell⁴⁴ from x-ray diffraction for terbium do not show discontinuities in the lattice parameters a , b , and c at T_C . However, the x-ray diffraction measurements of Finkel *et al.*⁴⁵ for terbium show a discontinuity (c_2-c_1) of about -1.1×10^{-3} Å in the parameter c at T_C and a discontinuous change in atomic volume (v_2-v_1) of about -5.4×10^{-3} Å³ at T_C . Recent b axis thermal-expansion measurements of White⁴⁶ on a high-purity single crystal of terbium indicated a discontinuity of about +0.01% in the length of the crystal along the b axis. However, because of the presence of magnetic domains this may not be a true measure of the change of lattice parameter. Darnell and Moore⁴⁷ and Finkel and Vorobev⁴⁸ have measured the lattice parameters of dysprosium from x-ray diffraction studies. They observed discontinuities in the lattice parameters at T_C ;

TABLE VIII. Our estimates of the latent heats of terbium and dysprosium at T_C obtained from Eqs. (A11) and (A12).

	Equation	Parameters	T_C (K)	L (J mol ⁻¹)
Tb	(A11)	Uniaxial stress ^a c -axis strain change ^b	221	33.7
Tb	(A11)	Uniaxial stress ^a b -axis strain change ^c	221	7.5
Tb	(A12)	Hydrostatic pressure ^d volume change ^b	221	57.8
Dy	(A11)	Uniaxial stress ^a c -axis strain change ^c	85	28.5
Dy	(A11)	Uniaxial stress ^a b -axis strain change ^c	85	74.5
Dy	(A11)	Uniaxial stress ^a a -axis strain change ^c	85	-224.4
Dy	(A11)	Uniaxial stress ^a c -axis strain change ^f	85	22.2
Dy	(A11)	Uniaxial stress ^a b -axis strain change ^f	85	-22.4
Dy	(A11)	Uniaxial stress ^a a -axis strain change ^f	85	557.6
Dy	(A12)	Hydrostatic pressure ^d Volume change ^f	85	-254.7
Dy	(A12)	Hydrostatic pressure ^d Volume change ^c	85	33.9

^aBartholin *et al.* (Ref. 42).

^bFinkel *et al.* (Ref. 45).

^cWhite (Ref. 46).

^dBartholin and Bloch (Ref. 43).

^eDarnell and Moore (Ref. 47).

^fFinkel and Vorobev (Ref. 48).

their results are given in Table VII, and are seen to be in radical disagreement.

We have estimated the values of the latent heat associated with the discontinuous transitions at T_C of terbium and dysprosium from the above-mentioned results of various authors using the Eqs. (A11) and (A12); these estimates of the latent heat are summarized in Table VIII.

As can be seen in Table VIII, the values of the latent heat L estimated from the results of different authors do not agree, and in some cases unphysical negative values were obtained for L . Furthermore, none of the values of L given in Table VIII agrees with the values we obtained from specific-heat measurements for terbium¹⁷ ($L = 13.6 \pm 0.6 \text{ J mol}^{-1}$) and dysprosium ($L = 39.1 \pm 1.5 \text{ J mol}^{-1}$, Sec. IV B); only the value $L = 7.5 \text{ J mol}^{-1}$ for terbium estimated from recent b axis thermal-expansion measurements of White⁴⁶ and uniaxial stress measurements of Bartholin *et al.*⁴² and the value $L = 33.9 \text{ J mol}^{-1}$ for dysprosium estimated from the hydrostatic pressure measurement of Bartholin and Bloch⁴³ and the value of the volume change of Darnell and Moore⁴⁷ are in rough agreement with our result.

There are two possible reasons for the failure of the values of the latent heat estimated from Eq. (A11) to agree with the experimental values. The first is that the parameters used in the equations may not be accurate. We have already noted the discrepancies in the measurements of lattice parameters. Coe and Paterson³⁶ have pointed out that the relation

$$\frac{\partial T_C}{\partial p} = \sum_i \frac{\partial T_C}{\partial \sigma^{ii}}$$

should be valid, and found it to be so for the α - β structural transition in quartz. The data in Table VI do not satisfy this relation and for this reason must be considered questionable. The second reason is that the arguments that lead to Eqs. (A10) and (A11) assume that the two-phase sample is subjected to constant and uniform magnetic field and stress. This might be so for the magnetic field case in the event that a domain structure arose that caused the field to be effectively zero in that part of the sample that was in the ferromagnetic phase. A state of uniform stress is less likely in view of the strains that occur at the transition.

It should be noted that McEwen⁴⁹ and McKenna¹⁸ have calculated the latent heat at T_C of dysprosium and terbium, respectively, using Eq. (A12). McEwen used the values $\Delta v = v_2 - v_1 = 0.2\%$ (should be 0.29%) of Finkel and Vorobev⁴⁸ and $\partial T_C / \partial \sigma^{bb} = 9.9 \text{ K/kbar}$ of Bartholin *et al.*⁴² and obtained $L = 33 \text{ J mol}^{-1}$ for dysprosium. Adopting the same approach, McKenna used the values $\Delta v = 0.017\%$ (should be -0.017%) of Finkel *et al.*⁴⁵ and $\partial T_C / \partial \sigma^{bb} = 5.7 \text{ K/kbar}$ of Bartholin *et al.*⁴² and obtained $L = 13 \text{ J mol}^{-1}$ (this should be -13 J mol^{-1}) for terbium. However, we consider that the above estimates of L obtained by McEwen⁴⁹ and McKenna¹⁸ are incorrect because they used the axial stress dependence of T_C , instead of hydrostatic pressure dependence of T_C in Eq. (A12).

*Present address: Department of Physics, University of New South Wales, Faculty of Military Studies, Duntroon, ACT 2600.

¹K. D. Jayasuriya, A. M. Stewart, S. J. Campbell, and E. S. R. Gopal, *J. Phys. F* **14**, 1725 (1984).

²K. D. Jayasuriya, S. J. Campbell, and A. M. Stewart, *J. Phys. F* **15**, 225 (1985).

³B. Coqblin, *The Electronic Structure of Rare Earth Metals and Alloys: The Magnetic Heavy Rare Earths* (Academic, London, 1977).

⁴J. G. Dash, R. D. Taylor, and P. P. Craig, in *Proceedings of the Seventh International Conference on Low Temperature Physics* (Toronto Press, Toronto, 1961).

⁵O. V. Lounasmaa and R. A. Guenther, *Phys. Rev.* **126**, 1357 (1962).

⁶O. V. Lounasmaa and L. J. Sundstrom, *Phys. Rev.* **150**, 399 (1966).

⁷L. J. Sundstrom, in *Handbook on the Physics and Chemistry of Rare Earths*, edited by K. A. Gschneidner, Jr. and L. R. Eyring (North-Holland, Amsterdam, 1978), Vol. I.

⁸M. Griffel, R. E. Skochdopole, and F. H. Spedding, *J. Chem. Phys.* **25**, 75 (1956).

⁹E. B. Amitin, Y. A. Kovalevskaya, F. S. Rakhmenknlov, and I. E. Paukov, *Fiz. Tverd. Tela (Leningrad)* **12**, 774 (1970) [*Sov. Phys.—Solid State* **12**, 599 (1970)].

¹⁰F. L. Lederman and M. B. Salamon, *Solid State Commun.* **15**, 1373 (1974).

¹¹T. J. McKenna, S. J. Campbell, D. H. Chaplin, and G. V. H. Wilson, *Solid State Commun.* **40**, 117 (1981).

¹²E. B. Amitin, V. G. Bessergenev, and Y. A. Kovalevskaya, *Zh. Eksp. Teor. Fiz.* **84**, 205 (1983) [*Sov. Phys.—JETP* **57**, 117 (1983)].

¹³B. J. Beaudry and K. A. Gschneidner, Jr., in *Handbook on the Physics and Chemistry of Rare Earths*, edited by K. A. Gschneidner, Jr. and L. R. Eyring (North-Holland, Amsterdam, 1978), Vol. I.

¹⁴T. J. McKenna, S. J. Campbell, D. H. Chaplin, and G. V. H. Wilson, *Phys. Status Solidi A* **75**, 421 (1983); S. B. Palmer, *J. Phys. F* **5**, 2370 (1975).

¹⁵Z. Barak and M. B. Walker, *Phys. Rev. B* **25**, 1969 (1982).

¹⁶D. A. Tindall and M. O. Steinitz, *J. Phys. F* **13**, L71 (1983).

¹⁷K. D. Jayasuriya, S. J. Campbell, A. M. Stewart, and E. S. R. Gopal, *J. Magn. Magn. Mater.* **31–34**, 1055 (1983).

¹⁸T. J. McKenna, Ph.D. thesis, University of New South Wales, 1980.

¹⁹L. D. Jennings, R. E. Miller, and F. H. Spedding, *J. Chem. Phys.* **33**, 1849 (1960).

²⁰P. R. Bevington, *Data Reduction and Error Analysis for Physical Sciences* (McGraw-Hill, New York, 1969).

²¹M. Barmatz, P. C. Hohenberg, and A. Kornblit, *Phys. Rev. B* **12**, 1947 (1975); A. B. Harris, *J. Phys. C* **7**, 1671 (1974).

²²I. S. Williams, E. S. R. Gopal, and R. Street, *Phys. Status Solidi A* **67**, 83 (1981).

²³A. Kumar, H. R. Krishnamurthy, and E. S. R. Gopal, *Phys. Rep.* **98**, 57 (1983).

²⁴F. L. Lederman, Ph.D. thesis, University of Illinois, 1975. (We are grateful to Professor M. B. Salamon for sending details of data reported in Ref. 10.)

- ²⁵M. B. Salamon, *Solid State Commun.* **13**, 1741 (1973).
- ²⁶M. Kopp (private communication).
- ²⁷T. J. McKenna, S. J. Campbell, D. H. Chaplin, and G. V. H. Wilson, *J. Magn. Magn. Mater.* **20**, 207 (1980).
- ²⁸E. B. Amitin, V. G. Bessergenev, L. A. Boyarskii, Y. A. Kovalevskaya, O. D. Christyakov, and E. M. Savitskii, *Fiz. Tverd. Tela (Leningrad)* **24**, 245 (1982) [*Sov. Phys.—Solid State* **24**, 136 (1982)].
- ²⁹I. Balberg and A. Maman, *Physica (Utrecht)* **96B**, 54 (1979).
- ³⁰G. Malmstrom and D. J. W. Geldart, *Phys. Rev. B* **21**, 1133 (1980).
- ³¹K. V. Rao, O. Rapp, C. Johannesson, D. J. W. Geldart, and T. G. Richard, *J. Phys. C* **8**, 2135 (1975).
- ³²M. Droz and M. S. Coutinho-Filho, in *Magnetism and Magnetic Materials—1975, Philadelphia*, proceedings of the 21st Annual Conference on Magnetism and Magnetic Materials, edited by J. J. Becker, G. H. Lander, and J. J. Rhyne (AIP, New York, 1976).
- ³³P. Bak and D. Mukamel, *Phys. Rev. B* **13**, 5086 (1976).
- ³⁴W. Selke, *Z. Phys. B* **29**, 133 (1978).
- ³⁵M. N. Barber, *J. Phys. A* **15**, 915 (1982).
- ³⁶A. B. Pippard, *The Elements of Classical Thermodynamics* (Cambridge University Press, London, 1966); R. S. Coe and M. S. Paterson, *J. Geophys. Res.* **74**, 4921 (1969).
- ³⁷D. R. Behrendt, S. Legvold, and F. H. Spedding, *Phys. Rev.* **109**, 1544 (1958).
- ³⁸J. L. Feron, Ph.D. thesis, Grenoble, 1969 (see Ref. 3).
- ³⁹D. Fort, D. W. Jones, E. D. Greenough, and N. F. Hettiarachchi, *J. Magn. Magn. Mater.* **23**, 1 (1981).
- ⁴⁰D. M. Hegland, S. Legvold, and F. H. Spedding, *Phys. Rev.* **131**, 158 (1963).
- ⁴¹R. D. Greenough and N. F. Hettiarachchi, *J. Magn. Magn. Mater.* **31—34**, 178 (1983).
- ⁴²H. Bartholin, J. Beille, D. Bloch, P. Boutron, and J. L. Feron, *J. Appl. Phys.* **42**, 1679 (1971).
- ⁴³H. Bartholin and D. Bloch, *J. Phys. Chem. Solids* **29**, 1063 (1968).
- ⁴⁴F. J. Darnell, *Phys. Rev.* **130**, 1825 (1963).
- ⁴⁵V. A. Finkel, Y. N. Smirnov, and V. V. Vorobev, *Zh. Eksp. Teor. Fiz.* **51**, 32 (1966) [*Sov. Phys.—JETP* **24**, 21 (1967)].
- ⁴⁶G. K. White (private communication).
- ⁴⁷F. J. Darnell and E. P. Moore, *J. Appl. Phys.* **34**, 1337 (1963).
- ⁴⁸V. A. Finkel and V. V. Vorobev, *Zh. Eksp. Teor. Fiz.* **51**, 786 (1966) [*Sov. Phys.—JETP* **24**, 524 (1967)].
- ⁴⁹K. A. McEwen, in *Handbook on the Physics and Chemistry of Rare Earths*, edited by K. A. Gschneidner, Jr. and L. R. Eyring (North-Holland, Amsterdam, 1978).